

Contact Interactions of Polyisobutylene Polymers

D. D. Deshpande* and C. S. Prabhu

Department of Chemistry, Indian Institute of Technology, Powai, Bombay 400 076, India. Received August 2, 1976

ABSTRACT: The heat of mixing at infinite dilution of three polyisobutylene polymers ($\bar{M}_n = 360, 1000, \text{ and } 1300$) with *n*-pentane, *n*-heptane, *n*-dodecane, *n*-hexadecane, benzene, cyclohexane, and carbon tetrachloride has been measured at 25 °C using a Tian Calvet conduction calorimeter. The values of the Flory's interaction parameter X_{12} are calculated from these heats. These values for *n*-alkanes are compared with those determined by Flory and collaborators. The observed variation in X_{12}/S_1 with chain length of solvents and of polymers is discussed in terms of molecular orientational order in these liquids.

Heats of mixing of polyisobutylene ($\bar{M}_v = 40\,000$) in various normal alkanes were determined calorimetrically by Delmas and Patterson.¹ With the exception of *n*-hexadecane, the heats of mixing of PIB + *n*-alkanes are negative but become less negative with increase of the chain length of the alkane. In the Flory model^{2,3} the free volume or equation of state term gives a negative contribution to the heat of mixing as against a positive contribution arising out of contact interaction term containing the X_{12} parameter. When the chain length of the solvent is increased, the negative contribution from the free volume term diminishes and ultimately the heat of mixing will be positive as in the case of PIB + hexadecane. As the nature of the solute–solvent interaction is uniform in such a series, X_{12} might be expected to be similar for all PIB + *n*-alkane systems. However, the X_{12} parameter, calculated from the heats of mixing data, is found to decrease with the increase of chain length⁴ and this behavior is attributed to the lower van der Waals interactions of methyl end groups of the alkane with the polymer segment. This explanation is not consistent, however, with the experimental heats of mixing of *n*-alkanes and branched alkanes with several solutes, and *n*-alkanes usually show large positive heats while branched alkanes show low or negative heats. It was therefore argued by Patterson and co-workers in a series of papers that this discrepancy is not merely due to an incorrect equation of state term in the corresponding states theory, but also of neglect of a contribution due to molecular orientational order of solvent, solute, or both.

Following Patterson⁵

$$\frac{X_{12}}{S_1} = \frac{X_{12}}{S_1} (\text{force fields}) + \frac{X_{12}}{S_1} (\text{orientation}) \quad (1)$$

where the first term on the right-hand side of this equation merely depends on the difference of chemical nature of components of solution and not on their molecular size or shape (S_1 is the surface to volume ratio of the solvent) and would therefore be independent of the chain length of the solvent. On the other hand, the second term (X_{12}/S_1)(orientation) will vary with the chain length of molecules. This contribution can be empirically related to orientational order parameters J_1 and J_2 of solvent and solute respectively through the relation⁵

$$\frac{X_{12}}{S_1} (\text{orientation}) = \text{constant} \times (J_1^{1/2} - J_2^{1/2})^2 \quad (2)$$

In this paper we have reported the heats of mixing of three different samples of polyisobutylene of low molecular mass in various *n*-alkanes and in solvents with spherical molecules in order to determine the effect of chain length of polymer on heats of mixing and on X_{12} .

Experimental Section

Materials. PIB samples are from British Petroleum Chemicals International Limited with Hyvis No. 05, 10, and 30. Number average

molecular masses are $\bar{M}_n = 360, 1000, \text{ and } 1300$, respectively, as reported by the manufacturers. The \bar{M}_v values experimentally measured by us are 700, 2000, 2500, respectively. The IR spectrum does not give evidence for the presence of any double bond in the sample with $\bar{M}_n = 360$. The IR spectra of the other two samples show the presence of $-\text{CH}_2-\text{C}(\text{CH}_3)=\text{C}(\text{CH}_3)_2$ group at the end of the chain. The manufacturers report that such a group would be only at one end of the chain. The *n*-pentane, *n*-heptane, benzene, cyclohexane, and carbon tetrachloride were of analytical reagent grade obtained either from E. Merck or from British Drug House. They were further purified by standard methods given by Weissberger⁶ and solvent purity has been tested by GLC analysis. Dodecane and hexadecane were of Fluka AG and were used without further purification. Their reported purity is greater than 99%.

Calorimeter. Heats of mixing were determined using a Tian Calvet monocell conduction calorimeter constructed by us. The details of its working principle are described elsewhere.⁷ It consists of a Pyrex glass cell, cylindrical in shape, and slides into an aluminium cylindrical cavity. The outer surface of the cavity is symmetrically surrounded by 160 thermojunctions made of copper and constantan. A heavy cylindrical block of brass, closed at the bottom, acts as a sink for the heat flow. The top portion of the sink is provided with a circular opening for the introduction of the experimental cell. The assembly is fitted in an adiabatic flask which can be rotated around a horizontal axle for the purpose of mixing the two components. Fluctuations in the ambient temperature are minimized by housing the calorimeter in an air-conditioned room. Any minute heat loss occurring constantly through the flask is compensated by joule heating. For this purpose heater wires are wound round the sink. A stabilized variable dc supply is used for the electrical heater.

The experimental Pyrex glass cell consists of two unequal compartments separated by a Teflon plug with a small quantity of mercury over it. The bottom end is flat and closed and to the top is fitted a rotaflo stopper. The total volume available for the solution is about 25 ml. This volume can be varied by introducing mercury or glass rods in the cell. Any heat contribution which might occur due to friction of dummy glass rods or mercury is measured separately. This contribution was not more than 0.2 J for a period of 3 h. For all our systems the mixing process was complete within this period.

Weighed amounts of polymers and solvents were introduced in lower and upper compartments, respectively. The vapor space was kept as small as possible. The rotaflo stopper completely seals off the upper compartment. The cell is then introduced in the cavity and the system is then thermally insulated from the surroundings. Attainment of thermal equilibrium takes about 4 h. The thermopile output can be electrically amplified up to 100 times. The chart speed of the recorder is 120 mm/h and the range -2.5 to $+2.5$ mV (centre zero). The calibration of the apparatus is done by joule heating and the area under the curve is measured by a planimeter. The smallest heat measurable is of the order of 0.25 J within 2 to 3%.

Using the constants given in Table I, heats of mixing for two systems, cyclohexane (1) + carbon tetrachloride (2) and benzene (1) + carbon tetrachloride (2), were measured at 25 °C. These values agreed well with the literature.^{8,9} Figure 1 shows the plot of literature and experimental values of heat of mixing for the first system.

For each polymer and solvent system heats of mixing were measured at four different concentrations expressed in weight fractions of polymer ranging from 0.05 to 0.2 and 0.1 to 0.4 depending on the solubilities. The heat of mixing at infinite dilution $\Delta h^M(\infty)$ is then calculated from

$$\Delta h^M(\infty) = \Delta h^M/W_1 \quad (3)$$

where W_1 is the weight fraction of the solvent.

Table I
Calibration Constants of the Calorimeter at 25 °C

| | | | | | |
|-------------------|-------|------|------|-------|-------|
| Amplifier gain | 1 | 5 | 10 | 50 | 100 |
| J/cm ² | 12.85 | 2.55 | 1.25 | 0.252 | 0.120 |

Table II
Characteristic Parameters and Reduced Variables for PIB Samples at 25 °C

| | PIB 05 | PIB 10 | PIB 30 | PIB ^a |
|--|--------|--------|--------|------------------|
| \bar{M}_n | 360 | 1000 | 1300 | |
| \bar{M}_v | 700 | 2000 | 2500 | |
| v_{sp} , cm ³ g ⁻¹ | 1.1876 | 1.1270 | 1.1160 | 1.0910 |
| $\alpha \times 10^4$, deg ⁻¹ | 7.79 | 6.32 | 5.90 | 5.55 |
| αT | 4.31 | 5.31 | 5.70 | 6.05 |
| \bar{v} | 1.2004 | 1.1670 | 1.1571 | 1.1487 |
| v_{sp}^* , cm ³ g ⁻¹ | 0.9883 | 0.9674 | 0.9645 | 0.9493 |
| $\bar{T} \times 10^2$ | 4.92 | 4.30 | 4.10 | 3.93 |
| P^* , J cm ³ | 448 | 448 | 448 | 448 |

^a B. E. Eichinger and P. J. Flory, *Macromolecules*, **1**, 286 (1968).

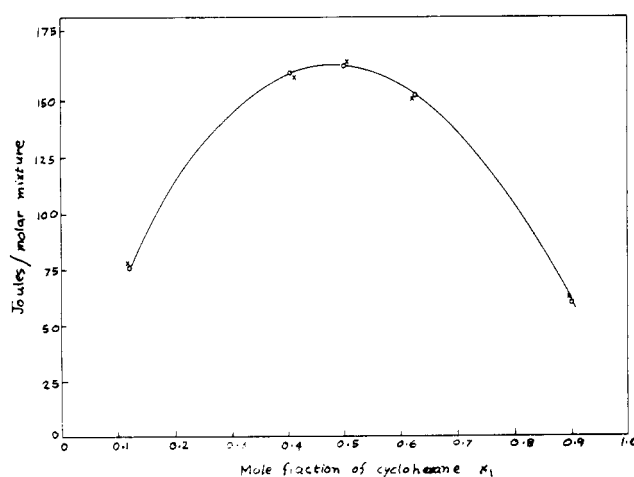


Figure 1. Comparison of heat of mixing for the system cyclohexane (1) + carbon tetrachloride (2) at 25 °C expressed per molar mixture and plotted against X_1 , the mole fraction of cyclohexane: (O) literature values; (X) experimental values.

Results

The Flory's parameter X_{12} is calculated using the expression³

$$\Delta h^{M(\infty)} = v_{2,sp}^* X_{12} \frac{S_2}{S_1} (1 + \alpha_1 T) \bar{v}_1^{-1} + P_2^* v_{2,sp}^* \left[\bar{v}_2 - \bar{v}_1 - \frac{(\bar{T}_1 - \bar{T}_2) \alpha_1 T}{\bar{v}_1 \bar{T}_1} \right] \quad (4)$$

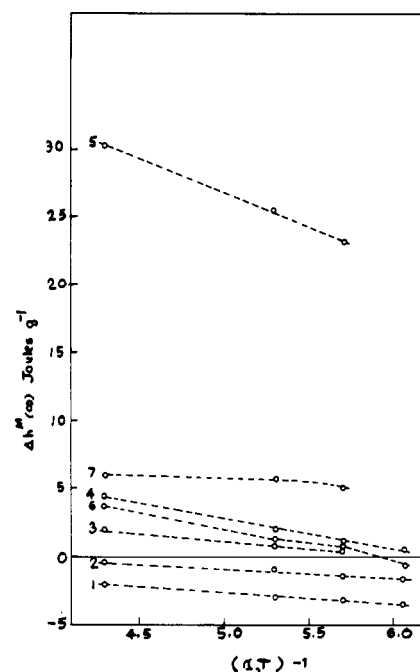


Figure 2. Directly measured values $\Delta h^{M(\infty)}$ for polyisobutylene polymers with solvents at 25 °C plotted against $(\alpha_2 T)^{-1}$. For PIB $\bar{M}_v \approx 40\,000$, the values are taken from ref 4. (Numbers at the left-hand side of the curves refer to solvent, see text.)

Here v^* is the characteristic specific volume, P^* is characteristic pressure, α is the thermal expansion coefficient, \bar{v} and \bar{T} the reduced volume and reduced temperature, and subscripts 1 and 2 stand for solvent and solute.

The characteristic parameters and reduced variable v^* , \bar{v} , and \bar{T} for polymers are calculated from the specific volumes v_{sp} and the thermal expansion coefficient α at 25 °C and at 1 atm. These values may be considered to hold good at zero pressure without appreciable error. The values for alkanes are at zero pressure reported by Flory et al.¹⁰ and for spherical molecules at 1 atm.¹¹ The following expressions are used which are in accordance with the Flory theory.

$$\bar{v} = 1 + \frac{\alpha T}{3(1 + \alpha T)}$$

$$\bar{T} = \frac{\bar{v}^{1/3} - 1}{\bar{v}^{4/3}}$$

$$\bar{v} = v_{sp}/v_{sp}^*$$

$$\bar{T} = T/T^*$$

v_{sp} and α for solutes were determined by using both a specific gravity bottle and a pycnometer. Surface to volume ratios S_2 for polymers were calculated as per Flory's procedure⁴ and

Table III
Properties of Solvents Used for Mixing at 25 °C (from References 10 and 11)

| No. | Solvents | $\alpha \times 10^3$, deg ⁻¹ | \bar{v} | $\bar{T} \times 10^2$ | J^d | S_1 , Å ⁻¹ |
|-----|----------------------|--|-----------|-----------------------|-------|-------------------------|
| 1 | <i>n</i> -Pentane | 1.610 | 1.3607 | 7.170 | 0.08 | 1.08 ^a |
| 2 | <i>n</i> -Heptane | 1.253 | 1.2973 | 6.405 | 0.30 | 1.00 ^a |
| 3 | <i>n</i> -Dodecane | 0.974 | 1.2420 | 5.610 | 0.82 | 0.93 ^a |
| 4 | <i>n</i> -Hexadecane | 0.901 | 1.2270 | 5.371 | 1.25 | 0.90 ^a |
| 5 | Benzene | 1.223 | 1.2916 | 6.330 | 0 | 0.96 ^b |
| 6 | Cyclohexane | 1.217 | 1.2905 | 6.310 | 0 | 0.91 ^b |
| 7 | Carbon tetrachloride | 1.229 | 1.2927 | 6.344 | 0 | 0.96 ^b |

^a V. T. Lam, P. Picker, D. Patterson, and P. Tancrede, *J. Chem. Soc., Faraday Trans. 2*, **70**, 1467 (1974). ^b Reference 11.

Table IV
Interpretation of Enthalpies of Mixing of PIB and Its Low Oligomers with Solvents
(Data for PIB, $\bar{M}_v \approx 40\,000$, are from Reference 4)

| No. | Solvent | $\Delta h^M(\infty), \text{J g}^{-1}$ | | | | S_2/S_1 | | | | $X_{12}, \text{J cm}^{-3}$ | | | |
|-----|----------------------------------|---------------------------------------|--------|--------|------------------|-----------|--------|--------|------------------|----------------------------|--------|--------|------------------|
| | | PIB 05 | PIB 10 | PIB 30 | PIB ^a | PIB 05 | PIB 10 | PIB 30 | PIB ^a | PIB 05 | PIB 10 | PIB 30 | PIB ^a |
| 1 | C ₅ | -1.90 | -2.90 | -3.20 | -3.6 | 0.552 | 0.541 | 0.539 | 0.53 | 6.1 | 9.5 | 10.9 | 11.7 |
| 2 | C ₇ | -0.48 | -0.96 | -1.38 | -1.8 | 0.596 | 0.584 | 0.582 | 0.57 | 2.4 | 4.6 | 5.1 | 5.3 |
| 3 | C ₁₂ | 1.91 | 0.67 | 0.54 | | 0.641 | 0.628 | 0.626 | 0.62 | 3.5 | 3.0 | 3.7 | |
| 4 | C ₁₆ | 4.47 | 2.12 | 0.98 | 0.45 | 0.662 | 0.649 | 0.647 | 0.64 | 6.8 | 4.4 | 3.2 | 2.8 |
| 5 | C ₆ H ₆ | 30.20 | 25.40 | 23.00 | | 0.621 | 0.608 | 0.606 | 0.60 | 49 | 46 | 44 | 42 |
| 6 | C-C ₆ H ₁₂ | 3.78 | 1.21 | 1.13 | -0.72 | 0.655 | 0.642 | 0.639 | 0.63 | 7.9 | 6.8 | 7.8 | 6.0 |
| 7 | CCl ₄ | 5.90 | 5.75 | 5.00 | | 0.621 | 0.608 | 0.606 | 0.60 | 12.4 | 14.8 | 14.8 | |

^a $\bar{M}_v = 40\,000$.

Table V
 X_{12}/S_1 for Solvents + PIB Systems

| Solvent | $X_{12}/S_1, \text{J cm}^{-3} \text{Å}$ | | | |
|----------------------------------|---|--------|--------|------------------|
| | PIB 05 | PIB 10 | PIB 30 | PIB ^a |
| C ₅ | 5.7 | 8.8 | 10.1 | 10.8 |
| C ₇ | 2.4 | 4.6 | 5.1 | 5.3 |
| C ₁₂ | 3.8 | 3.2 | 3.9 | |
| C ₁₆ | 7.5 | 4.9 | 3.6 | 2.4 |
| C ₆ H ₆ | 51 | 47.9 | 45.8 | 43.8 |
| C-C ₆ H ₁₂ | 8.7 | 7.5 | 8.6 | 6.6 |
| CCl ₄ | 12.9 | 15.4 | 15.4 | |

^a $\bar{M}_v = 40\,000$.

values were given for diameter and segment length; v^* was calculated from our data on thermal expansion coefficient α for each sample.

Discussion

$\Delta h^M(\infty)$ values for PIB and its low molecular mass oligomers are plotted against $(\alpha_2 T)^{-1}$ in Figure 2. There is a decrease in $\Delta h^M(\infty)$ with increasing molecular mass of PIB for all solvents. For all PIB samples in n -C₅ and n -C₇, $\Delta h^M(\infty)$ is negative. For these solvents the ordering is nearly zero and thus negative $\Delta h^M(\infty)$ is ascribed to the predominant contribution of the free volume term. The X_{12} parameter calculated from eq 4 is found to be positive for all the systems and it is expected of systems of nonpolar molecules that solute-solvent interactions are weaker than the mean of the solute-solute and solvent-solvent interactions. From Table IV it will be revealed that the values of X_{12} for systems with spherical molecules like cyclohexane and carbon tetrachloride do not vary appreciably with the chain length of the polymer. Since the orientational order in these spherical molecules is zero, it may be assumed that there is either negligible or a constant but nonzero amount of order in all the PIB samples. This, however, would need some experimental support like that from measurement of optical anisotropy.

The X_{12}/S_1 value in Table V increases with \bar{M}_n for PIB + n -C₅, is constant for n -C₁₂, and decreases with \bar{M}_n for n -C₁₆. For n -C₅, where the free volume term in $\Delta h^M(\infty)$ data is important, it seems that this contribution is overestimated by the Flory theory, and the variation of X_{12}/S_1 with \bar{M}_n compensates for this error. However, for n -C₁₆ where the free volume is much less significant, another effect becomes important. This is the breaking up of orientational order in the n -C₁₆ by PIB. The decrease of X_{12}/S_1 with increase of PIB chain length can be explained if one assumes that the breaking

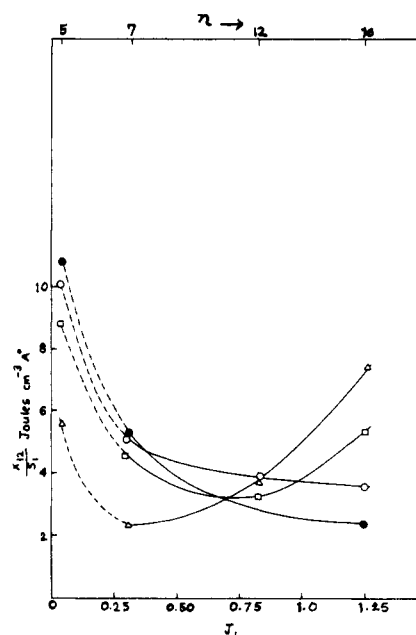


Figure 3. Values of the X_{12}/S_1 parameter against the molecular orientation parameter J_1 of solvents. J_2 in eq 2 is put equal to zero: (Δ) PIB 05, (\square) PIB 10, (\circ) PIB 30, (\bullet) PIB $\bar{M}_v \approx 40\,000$.

up becomes less effective as the molecular weight of the PIB increases. If the variation of X_{12}/S_1 for n -C₁₆ with the PIB's of different chain length is due to their different order destroying efficiencies, then a highly branched C₁₆ showing no order should give a small constant X_{12}/S_1 value. This, however, would need experimental support.

In Figure 3 the plot of X_{12}/S_1 against J_1 is given. As expected from eq 2, straight lines should have been obtained for different PIB samples. We believe that the deviations are again due to overestimation of the free volume term for shorter alkanes and the inability of long polymer chains to destroy the orientational order in long alkanes. Also, the orientational order parameter J_2 for polymer may not be equal to zero. In order to see the effect of variation of S_2 for each of the PIB samples, $X_{12}S_2/S_1$ was calculated, but the trend of variation remained unaffected.

References and Notes

- (1) G. Delmas, D. Patterson, and T. Somcynsky, *J. Polym. Soc.*, **57**, 79 (1962).
- (2) B. E. Eichinger and P. J. Flory, *Trans. Faraday Soc.*, **64**, 2035 (1968).
- (3) D. W. Dreifus and D. Patterson, *Trans. Faraday Soc.*, **67**, 632 (1971).
- (4) P. J. Flory, J. L. Ellison, and B. E. Eichinger, *Macromolecules*, **1**, 282 (1968).

- (5) V. T. Lam, P. Picker, D. Patterson, and P. Tancrede, *J. Chem. Soc., Faraday Trans. 2*, **70**, 1476 (1974).
- (6) A. Weissberger, "Technique of Organic Chemistry", Vol. VII, Interscience, New York, N.Y., 1955.
- (7) E. Calvet and H. Prat, "Recent Progress in Microcalorimetry", Pergamon Press, New York, N.Y., 1963.
- (8) M. B. Ewing and K. N. Marsh, *J. Chem. Thermodyn.*, **2**, 352 (1970).
- (9) S. Murakami and G. C. Benzon, *J. Chem. Thermodyn.*, **1**, 565 (1969).
- (10) R. A. Orwoll, P. J. Flory, J. L. Ellenson, and B. E. Eichinger, *Macromolecules*, **1**, 283 (1968).
- (11) A. Abe and P. J. Flory, *J. Am. Chem. Soc.*, **87**, 1840 (1965).
- (12) P. Tancrede, D. Patterson, and V. T. Lam, *J. Chem. Soc., Faraday Trans. 2*, **71**, 994 (1975).

Neutron Scattering by Uniaxially Hot Stretched Polystyrene Samples

C. Picot,* ^{1a} R. Duplessix, D. Decker, ^{1a} H. Benoit, ^{1a} F. Boue, ^{1b}
J. P. Cotton, ^{1b} M. Daoud, ^{1b} B. Farnoux, ^{1b} G. Jannink, ^{1b} M. Nierlich, ^{1b}
A. J. de Vries, ^{1c} and P. Pincus ^{1d}

C.R.M., 67083 Strasbourg, France; Laboratory Léon Brillouin, CENS, 91120 Gif, sur Yvette, France; Centre de Recherche de la Croix de Berny, Rhône Poulenc Industries, 92160 Antony, France; Collège de France, 75231 Paris, France; and Laboratory de Physique des Solides, Université Paris Sud, 91405 Orsay, France.
Received January 23, 1976

ABSTRACT: Neutron small-angle scattering experiments by tagged polystyrene films hot stretched and subsequently quenched are discussed in terms of coil deformation. The parameters which are varied in this experiment are the extension ratio λ , the hot stretch temperature T_1 , and in one case a partial recovery between the stretch and quench phases. The nature of the deformation is examined at different pair correlation distances r , in between R'' the coil size in the stretch direction and l the step length. Below a length r^* , we find deviations to the affine deformation in the longitudinal direction. This deviation increases, at given λ , with the hot stretch temperature and shows how the loss of molecular orientation observed in birefringence is compatible with a total recovery of the sample after annealing.

(I) Uniaxial Stretching

In this report we examine the deformation of coils in uniaxially hot stretched polystyrene films. The samples are films of lengths $L_0 \approx 3$ cm, made of a mixture of 99% protonated and 1% deuterated polystyrene ($M_w = 1.17 \times 10^5$). The molecular weight dispersion^{2a} is $M_w/M_n = 1.1$. At a given temperature T_1 above the glass transition T_G ($\sim 95^\circ\text{C}$), they are stretched with a velocity gradient $s(t) = (1/L(t)) dL(t)/dt$, where $L(t)$ is the length of the film at time t . Upon stretching, they are quenched at a temperature $T_2 \ll T_G$ while being maintained at the fixed end-to-end length L . A neutron small-angle scattering measurement is then made at room temperature. One sample, labeled Re, is allowed to relax before quenching by letting the end-to-end length decrease from \bar{L} to $\bar{L} = 0.95L$, at the temperature T_1 . Only thereafter is it frozen in and measured. The sequence of events is seen in Figure 1. The figure shows in fact the succession of a stretching phase in the time interval $(0, t_1)$ and a quench phase in the interval (t_2, t_3) . The time necessary to switch from one phase to the other is $(t_2 - t_1)$ and is kept as small as possible. During the time $(t_3 - t_1)$ the sample is kept at the fixed end-to-end length L at a temperature which decreases from T_1 but is still above T_G . The stress relaxes and therefore (t_1, t_3) will be called a stress relaxation phase. For sample Re, the stress relaxation is preceded by a strain relaxation phase.

Molecular orientation frozen in such samples has been measured by birefringence experiments^{2b,3} and was found to be dependent upon the stretch ratio $\lambda = L_0/L$ and the temperature T_1 . In particular, for a given λ , birefringence and consequently orientation decrease as T_1 increases. This observation is difficult to interpret, because the samples generally recover their initial length L_0 when annealed at a temperature greater or equal to T_1 after quenching. Thus on the macroscopic scale, the deformation is purely elastic (this was

not tested on our samples but is inferred³ from earlier hot stretch experiments with higher molecular weights). On the microscopic scale, there must on the contrary be a form of viscous deformation since molecular orientation is increasingly relaxed as the temperature is raised. We expect thus that the decomposition of the deformation^{2b}

$$\lambda - 1 = \lambda_i + \lambda_{he} + \lambda_v - 3 \quad (1)$$

into instantaneous, high elastic, and viscous deformations is not identically the same at different spatial scales. On the scale L , the last term is negligible with respect to the second and first terms in our experimental conditions. On the segment scale, the situation is very different. We expect from the scattering experiment to cover part of the intermediate situations because of the possibility of exploring reciprocal space by variation of the scattering angle. We can think of two types of coil deformation in the hot stretch phase.

(A) The deformation is *uniformly* affine,⁴ which amounts to saying that every vector $\mathbf{r}_{ij} = (x_{ij}, y_{ij}, z_{ij})$ joining two coil segments (i, j) is transformed into $\bar{\mathbf{r}}_{ij} = (\lambda x_{ij}, \lambda^{-1/2} y_{ij}, \lambda^{-1/2} z_{ij})$, the x axis being the uniaxial stretch direction. As a consequence, the average squared orientation of a coil segment with respect to the x axis (molecular orientation) is⁵

$$\langle \cos^2 \omega \rangle = 1/3 + 2(\lambda - 1)/5 + \dots \quad (\lambda - 1 \simeq \epsilon) \quad (2)$$

In this context, the result is of course totally independent of molecular weight.

(B) In another version,⁶ which applies to rubber elasticity, the affine deformation theory holds true only for distances separating effective cross links. Let \mathbf{r}_{pq} be such a vector. Then $\bar{\mathbf{r}}_{pq} = (\lambda x_{pq}, \lambda^{-1/2} y_{pq}, \lambda^{-1/2} z_{pq})$, but for all \mathbf{r}_{ij} inside \mathbf{r}_{pq} the deformation of the coil is determined by the response of a brownian chain to the constraint (p, q) . As a result, the average